The Effects of Field of View Size on the Control of Roll Motion

Robert V. Kenyon, *Member, IEEE*, and Edward W. Kneller, *Member, IEEE*

Abstract—**Human operator characteristics were measured during a fixed-base visual tracking task where the field of view (FOV) varied from 10° to 120°. Using the critical tracking (CT) task, five subjects were tested at 10°, 20°, 40°, 80°, and 120° FOV. The measured "effective" time delay (τ_e) declined exponentially as the FOV increased with two of five subjects nearly reaching their minimum τ_e with a FOV as small as 40° and three subjects reaching or nearly reaching their minimum τ_e with a FOV as small as 20°. The corresponding root-mean-squared (RMS) error followed a U-shaped curve with the majority of the RMS reduction at 40° FOV followed by an increase at 120°. This increase in RMS error was accompanied by the subjects' reports of increased task difficulty at 120° FOV. We hypothesize this increased RMS error was due to the episodic vection, reported only at this FOV, that briefly disoriented the subjects and thereby distracted them from the tracking task. A second experiment, where two subjects were tested at 10°, 40°, and 120° FOV, used a time-invariant plant to allow the measurement of human describing function parameters. The crossover frequency increased at least 5% and the RMS error dropped by at least 20% at a FOV of 40° or 120° compared to 10°. The results from these two experiments show that a FOV as small as 40° can produce performance improvements of the same magnitude as a FOV as large as 120°. The final experiment was identical to the CT experiment, described previously, except that only the central 10° of the scene rotated. Unexpectedly, performance was *best* at 10° and *poorest* at 40° and 80°, just the opposite of the previous two experiments. These results may be due to a "contrast motion vection" effect first reported during circularvection experiments.**

I. Introduction

A HUMAN operator's control over a vehicle with marginal stability characteristics can be enhanced by providing lead information to the operator. Such lead information can take the form of veridical motion sensed through the vestibular system or motion of the visual scene if a wide field of view (FOV) is available. Shirley and Young [22] showed that veridical motion cues during a pursuit tracking task provide high-frequency lead information that is most effective when controlling marginally stable systems. Levison and Junker [15] extended this work to show that veridcal motion cues can improve human performance more in a disturbance nulling tasks than in a target tracking task. Junker and Price [13] showed that a wide visual FOV and actual motion can have similar effects on an operator's performance. More recently, Hosman and van der Vaart [7], [8] found significant improvement in root-mean-squared (RMS) roll error when the subject used peripheral displays to supplement the central display during a tracking task. Analysis of the human operator describing function showed that the subject's crossover frequency remained constant but their phase margin increased by 90%, when both peripheral and central displays were used in a target following task, signifying a greater system stability.

This paper extends these studies and focuses on how much FOV is needed to extract performance improvements in a human operator during a fixed-base visual roll disturbance nulling task. We used the critical tracking (CT) task of Jex *et al.* [12] to measure the subject's "effective" time delay and other performance indexes with different FOV sizes ranging from 10° to 120°. Our results show that tracking performance increases with widening FOV sizes and that these performance gains begin to plateau at a FOV as small as 20°.

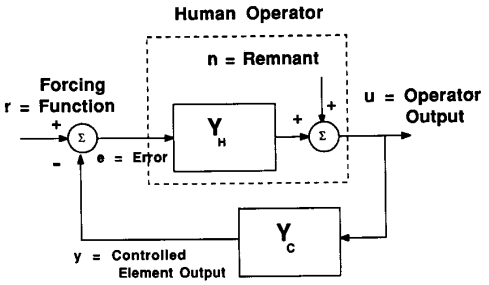

Fig. 1. General block diagram of the human operator as a controller in a feedback control system. In the critical tracking task, no external forcing function [$r = 0$] is applied; instead, the inherent noise of the human manual control system is used to disturb the system (disturbance nulling). In the subcritical task, a pseudorandom forcing function composed of 13 sinusoids is applied at the input [r] (compensatory tracking).

II. Methods

In these experiments, either a critical- or a subcritical-control plant was used for the roll dynamics of the visual scene. The subject acted as the controller in a feedback control system that included one of these first-order divergent control plants Y_c (see Fig. 1). The subject's task was to maintain the visual field at 0° roll angle.

Manuscript received August 13, 1991; revised July 2, 1992. The experiments were performed at the Man-Vehicle Laboratory, Department of Aeronautics and Astronautics, Massachusetts Institute of Technology, Cambridge. The work was supported by the U.S. Air Force under Contract F33615-83-0603-0020. Portions of these data were presented at the 1992 International Symposium for Information Display, Boston, MA, May 17–22.

R. V. Kenyon is with the Department of Electrical Engineering and Computer Science, University of Illinois, Chicago, IL 60680.

E. W. Kneller is with the U. S. Navy, Oceana NAS, Virginia Beach, VA 23451.

IEEE Log Number 9205791.

A. Critical Tracking Experiment

The critical tracking (CT) task was designed to identify the "effective" time delay of the human-operator τ_e [equation (5)], [12]. The subject's "effective" time delay includes the time that the central nervous system takes to process the visual information and send the neural signals to the muscles and time for the muscles to respond. The use of an increasingly unstable plant such as

$$Y_C = \frac{K_c}{Ts-1} = \frac{\lambda}{s-\lambda} \text{ where } \begin{cases} \lambda & =1/T \\ K_c & =1.0 \end{cases} \quad (1)$$

to drive roll motion of the scene requires the operator to adjust his time delay to maintain stability of the overall system. Since both the gain and phase margins vanish with increasing instability, the subject is not able to adopt lead or lag equalization, in which the subject trades off gain and phase in such a way as to optimize the control response [17]. Because of these factors, maintaining stability becomes increasingly difficult; and, at some value of control plant instability ($\lambda_c = 1/T_c$), the subject will lose control. In the critical control task, the input ($\boldsymbol{r}$) in Fig. 1 is zero and the operator's self-generated "noise" ($\boldsymbol{n}$), serves as the system's disturbance function. Jex *et al.* [12] showed that this critical instability level in the plant is a measure of the subject's "effective" time delay. In practice, the subject is not able to maintain a precise pure gain response and is likely to lose control at a plant instability time constant (T_c) that is less than τ_e because of the human operator's intrinsic variability and the inherent noise of the human operator.

1) Pacing Plant Instability: To measure ($\lambda_c = 1/T_c$) with reasonable accuracy, the rate at which λ changes must not greatly influence the outcome of the experiment. If the rate is too fast, the λ_c values may be too high due to λ increasing a significant amount after the subject has lost control, but before the scene has reached its maximum angle. Nevertheless, too slow an increase in λ would overly fatigue the subject.

The λ value used by the following control plant equation:

$$\theta(n) = [e^{\lambda h}]\theta(n-1) + e[^{\lambda h}-1]x(n-1)$$
$$\text{where } \begin{cases} h & =\Delta t \text{ (0.0667 s)} \\ x(n) & = \text{stick output} \\ \theta(n) & = \text{scene roll angle} \end{cases} \quad (2)$$

was increased using the equation

$$\lambda(n) = \lambda(n-1) + \Delta\lambda$$
$$\text{where } \begin{cases} \lambda(0) & = 1.5 \text{ rad} \\ \Delta\lambda & = 0.0075 \text{ rad then } 0.0020 \text{ rad} \end{cases} \quad (3)$$

based on a 15 Hz update rate. Initially, λ was incremented by 0.0075 rad per update cycle. Then, when λ was greater than 3.2 and the average absolute roll error over 2/3 s was greater than 13°, the increment decreased to 0.0020 rad until the subject lost control. The initial rapid increase in λ allowed the plant to move from a relatively stable level to the near critical level over a short time (20–40 s), thereby avoiding subject fatigue. The final slower increase prevented an overshoot of λ_c. When the roll angle reached ± 100°, the system was defined as uncontrollable, and the test was over. Roll angle limits as high as ± 200° were tested and found not too increase the critical instability level beyond the ± 100° criteria.

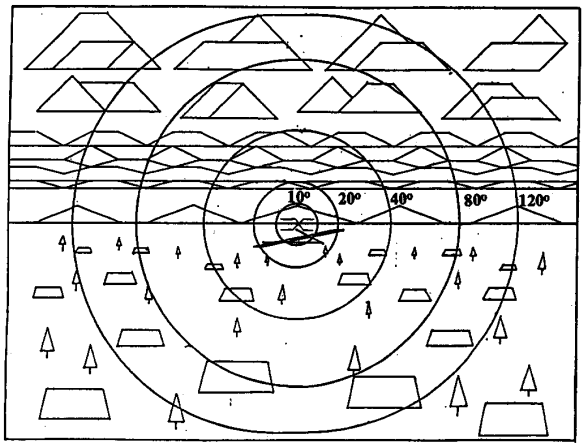

Fig. 2. A schematic representation of the out-the-window scene generated by the graphics workstation. The concentric rings show the extent of the scene visible at various field of view settings. A broken X in the center of the scene serves to indicate true horizontal, since it is fixed at 0° roll angle.

2) Visual Stimulus: A dedicated graphics workstation (Silicon Graphics IRIS 2400) was programmed to read and store the subject's control input and generate the out-the-window scene. The workstation displayed the scene on a 19 inch, 30 Hz interlaced color monitor with a resolution of 768 × 1024 red-green-blue (RGB) pixels (over the 120° FOV, each pixel measured 9.37 × 7.03-min arc). The scene viewed by the subject was a stylized landscape drawn in perspective (see Fig. 2) containing a well-defined horizon, high spatial frequency objects, and distant landscape features such as hills, clouds, and trees. Since there was only roll motion of the scene and the subject's head was fixed, there was no motion parallax to deal with in generating the perspective image. The 15-Hz update rate was sufficient to display smooth visual scene motion to the subject for virtually the entire experiment. The smooth motion would begin to appear choppy only at the very end of the CT experiments when the scene was out of control and about to crash. At this point in the experiment, the subject could not recover control of the system and this choppiness had no impact on the experimental results.

Two visual conditions were generated by the workstation. In both cases, a crosshairs symbol in the center of the display did not move with the scene and was fixed at 0° of roll to give the subject a reference from which to judge deviations of the moving scene from the desired 0° roll angle. In one condition, the entire visible FOV rolled according to the dynamics of the plant. In the other condition, only the central 10° of the entire visible FOV was controlled by the plant. The remaining portion of the visual scene was fixed at 0° of roll angle. For this stationary peripheral field case, the central 10° contained two semicircles forming an "artificial" horizon line that rolled according to the plant dynamics. The upper semicircle was colored yellow, and the lower, green with the fixed crosshairs superimposed over this figure. The remainder of the visual scene was the same as the previous condition.

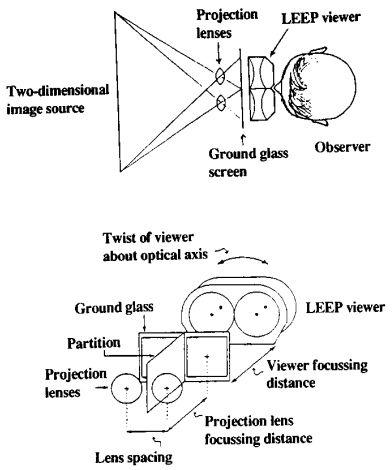

Fig. 3. The wide-FOV optical system used to provide the 120° FOV from the workstation's 19-in monitor (see text).

3) Field of View Optics: Subjects viewed the computer-generated scene on the cathode-ray tube (CRT) through an optical system that expanded its image over a diameter of 120° in both the horizontal and vertical axes (see Fig. 3). The optical system consisted of a binocular viewer (manufactured by Pop Optix Labs, Waltham, MA), a ground glass projection screen, and two projection and two Fresnel lenses. The sheet of ground glass (Rolyn Optics #55.3050) was placed 1 cm in front of the binocular viewer. The image from the CRT was projected onto this ground glass with two 80 mm projection lenses (Rolyn Optics #30.1451) producing two *duplicate* images with dimensions of 7 × 6 cm for each channel. A partition between the two lenses that extended to the ground glass screen prevented the two images from overlapping. To compensate for any fall-off in brightness in the periphery, a Fresnel lens ($f.l.$ = 10 cm; Rolyn Optics #16.7200) was placed against the far side of the ground glass in each channel so that light from the periphery was directed toward the eye.

A particular FOV was created by cutting circular holes in 2.5 × 4 in sections of black matte paper using the following equation to calculate the radius of the opening:

$$r = M(\theta - k\theta^3) \tag{4}$$

where θ is the angle in radians from the optical axis of the camera, r is the corresponding radial distance in centimeters from the center of the image with $k = 0.22$ rad^{-2} and $M = 3.7$ cm [9].

4) Protocol: Experiments were conducted on a fixed base in an 8 × 12 foot room that was well shielded from external sources of light and noise. Seated subjects used a chin rest to stabilize their heads, and they were shielded from all ambient light by a black felt cloth draped over the optical system and their heads. A simple two degree-of-freedom force-stick, used to control the *roll velocity* of the scene (Measurement Systems Model #435),[1] was mounted securely to the right-hand side of the subject's chair. A contoured armrest, also attached to the chair, was used to stabilize the forearm. Lateral force on the stick was converted to an analog voltage (±10 V range) that was antialiased with a first-order low-pass filter with a break frequency of 3.8 Hz. This analog signal with a voltage/force ratio of 22 m V/N was then samples at 15 Hz using an analog-to-digital (A/D) card installed in the workstation (Analog Devices DT772).[2] The sampled stick signal was converted to radians for use as a variable in control equation (2) using a scale factor of 0.09 rad/N.

Ten experimental conditions were used: five different FOV sizes (10°, 20°, 40°, 80°, and 120°) with either the moving or the stationary peripheral field. A single trial consisted of these ten conditions. Every subject ran six trials: three trials per day over two consecutive days. A trial lasted approximately 20–25 min, with a 5-m break between trials. Ordering effects on the data were minimized by balancing the presentation of the conditions within each trial.

5) Subjects and Training: Five males in good health, free of any obvious motor coordination anomalies, and with distant vision corrected to at least 20/20 served as subjects. Subject C used his left hand for writing but his right hand for throwing and other manual tasks. Subject B had fifty hours of visual flight rules (VFR) flight time in light aircraft, and subject E had 10 hours in advanced flight simulators.

Subjects were trained for three days before data collection began. First, familiarization runs were conducted with the subject viewing the CRT directly, i.e., without using the optical system. Subjects were instructed: a) to fixate on the center of the display,[3] b) to keep the displayed roll angle as close to 0° as possible, and c) to react quickly and accurately. Subjects nulled the roll motion with a lateral force in the direction of the scene's motion, a response similar to that of a pilot maintaining an aircraft at a wings-level attitude. Subjects applied the corrective force to a knob at the top of the control stick that was held between the thumb and index finger only.

After approximately ten trials viewing the CRT directly, subjects trained using the optical system. In the final stage of training, subjects ran at least one practice trial a day for three days. The stability of the critical λ value (λ_c) was used to measure whether a subject had been trained sufficiently. When the λ_c did not change more than ±0.2 rad/s over the last two trials, the training was stopped. Subjects C and D received the minimum amount of required training; subjects A, B, and E has at least ten practice trials each, since they were involved in the development of the experiment.

B. Subcritical Task Experiment

These experiments were conducted mainly to expand our results in the CT experiments, to examine trends in the human operator control, and to compare these results to other

[1] McDonnell and Jex [16], in a follow-up study to their original Critical Tracking Task, stated that displacement devices such as a self-centering displacement stick or a rotating knob, increase the subject's delay time due to limb positioning and muscle dynamics. A force stick with very little motion minimizes the subject's "effective" time delay.

[2] Since the computer could not generate a new visual scene faster than 15 Hz, this determined our sample rate for triggering data acquisition.

[3] During the practice trials, eye movements were monitored using electrooculography [25]. These data showed that fixation was confined to the central visual tracking symbol. This practice was discontinued in the data runs for reasons of subject comfort and fatigue and to reduce the complexity of the experiment.

published reports that used a time-invariant plant. It was not intended as an exhaustive study of human operator function with FOV changes.

Two changes to the moving periphery CT experiment were made to perform these experiments. First, to make the plant time-invariant, the value of λ was held constant for the entire trial. Next, to obtain human describing function parameters, an external forcing function was added at the input ($\mathbf{r}$) [17], [20]. The forcing function was designed to simulate a filtered white noise process and was generated by summing thirteen sinusoids. The fundamental frequency (ω_o) for the sinusoids had a base run time of 136.53 s corresponding to $\omega_o = 0.04602$ rad/s. The frequencies used were a prime harmonic of ω_o starting with the seventh harmonic (0.32, 0.59, 1.32, 1.69, 2.44, 3.35, 4.74, 6.85, 9.71, 13.49, and 19.30 rad/s). The total forcing function signal had a power spectral density (PSD) that was approximated by the first-order PSD function, with a break frequency of 0.5 rad/s. The phases of the sinusoids were set randomly.

Subjects B and E, who had the most experience with the CT experiments, were recruited for these experiments, and they completed ten practice trials at 120° FOV before starting the subcritical (SC) experiments. Subjects were tested at three FOV sizes: 10°, 40°, and 120°. Each used three λ values: 2.0 rad/s, 3.0 rad/s, and $\lambda_{\max}$ (a value that was 10% less than their best λ_c from the CT experiments). $\lambda_{\max}$ was 4.0 rad/s and 3.2 rad/s for subjects B and E, respectively. A trial consisted of one of each of these nine cases with two trials per subject. The tracking task for a single case lasted 2 min and 30 s. The subject was allowed to take a 5-min break during the trial. In all of these experiments, the motion of the entire visual scene was controlled by the subject; no stationary surround condition was used.

III. Data Analysis

A. Critical Tracking Experiment

Data analysis of the critical tracking experiment was based on four sets of measurements: two time constant measurements and two performance measurements based on the RMS of the visual roll error.

1) Time Constant Analysis: The time constant of the control element was measured at two specific points during the experiment: a) the point where $\Delta\lambda$ changed from fast to slow, called the "transition time constant" (T_t), and b) the point where the subject lost control of the scene, called the "critical time constant" (T_c). The value of T_t is a measure of the difficulty of the task prior to approaching T_c. Since $\Delta\lambda$ cannot be changed until λ reaches a minimum value of 3.2 rad/s, T_t had a maximum value of 0.3125 s (indicated in Fig. 4 by the line labeled "maximum transition"). The T_c value represents an estimate of the subject's "effective" time delay τ_e.

2) Performance Analysis: Two performance values, called Stage-1 and Stage-2 RMS error, were calculated for each data set. The Stage-1 value was obtained by computing the RMS of 226 roll error samples taken from the beginning of the test, when $\lambda = 1.5$ rad/s, to the point where $\lambda = 3.2$ rad/s, a total of 15.1 s (60–70% of the total experiment duration). Since the plant instability was applied uniformly for all experiments and independently of the subject's performance, these Stage-1 error values can be compared within and across subjects at different FOV settings.

The Stage-2 value was obtained by computing the RMS of roll error for data collected when $\lambda = 3.2$ rad/s to the end of the test. Since $\Delta\lambda$ changed from high to low at some point in this interval, the slower increase in λ caused the number of data points between T_t and T_c to increase by a factor of 3.75 [0.0075/0.0020 from (3)] over that which would have resulted if $\Delta\lambda$ remained high. This increase in the number of data points was compensated by multiplying the sum-of-squares value computed for the data collected up to T_t by 3.75 before adding to the sum-of-squares value obtained for the rest of the data. To compute the RMS, the total number of data points was increased by 3.75 times the number of samples up to T_t. The rationale was that the subject would produce roll error values of the same magnitude as those that were collected during the faster rate only more of them. The net effect was to approximate the set of data that would have resulted if $\Delta\lambda$ had the slower rate for the entire experiment instead of switching from fast to slow at T_t.

Furthermore, the duration of the period between $\lambda = 3.2$ and the end of the test was variable and dependent on the λ_c value. When calculating the mean and standard deviation of the six individual Stage-2 values of each experimental condition, each individual Stage-2 value was weighted by the actual number of roll error measurements from which the value was calculated. Therefore, Stage-2 values from tests that lasted a longer time affected the mean and standard deviation more than Stage-2 values from tests that lasted a shorter time.

B. Subcritical Tracking Experiment

The describing function of the human operator Y_h was calculated from the subject's input/output data using spectral analysis [17]. This analysis used the fast Fourier transform (FFT) to measure the correlation between the subject's output and input signals. The FFT analysis used a base period of 2048 data points, because it was the same as that used by the forcing function's sinusoids. The resulting Y_h was multiplied by Y_c to produce the open-loop transfer function of the system $Y_h Y_c$. This data was converted to a Bode plot to estimate the system's phase margin and crossover frequency assuming a simple crossover model for the open-loop system [17]:

$$Y_H Y_C = \frac{K_c}{j\omega} e^{-j\omega\tau_e} \tag{5}$$

where $K_c = \omega_c$ at the crossover frequency $\omega = \omega_c$. The crossover frequency and phase margin values were estimated directly from the bode plots by interpolating through the calculated gain and phase values. CT experiment Stage-1 and Stage-2 RMS error, and time

1) Statistics: Nonparametric statistics were used to analyze

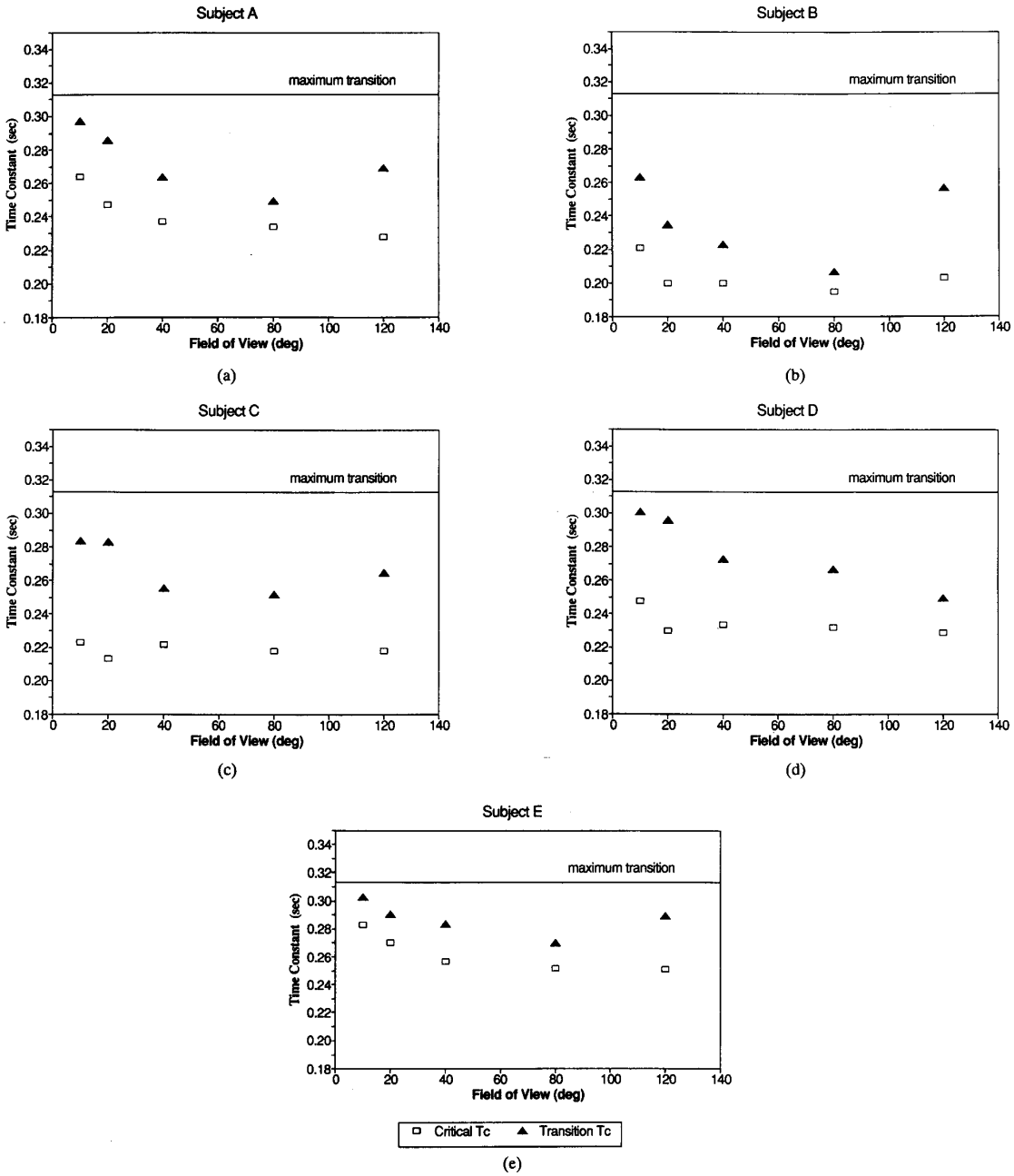

Fig. 4. Mean time constant values for all subjects versus FOV for the CT task with the peripheral field moving. The critical time constant (T_c) is represented by the open boxes and the transition time constant (T_t) by the filled triangles. The line marked "maximum transition" represents the maximum time constant value at which $\Delta\lambda$ changed from high to low, indicating an approach to critical λ (λ_c).

the possible differences between the experimental cases. Due to the low number of samples, the usual parametric statistics were not valid. A Mann–Whitney test was performed on the constant values within each subject. The Mann–Whitney test is similar to the t-test, but it makes no assumptions about variance and distributions. However, it is not as powerful a test as the t-test [21].

IV. Results

A. CT Experiment

The open-box symbols in Fig. 4 represent the mean critical time constant[4] (T_c) values for five subjects with the moving

[4]or "effective" time delay (τ_e) estimate.

visual scene condition. Although each subject had a different minimum T_c value indicative of differences in their ability to perform the task, the 10° FOV produced the longest T_c in all of our subjects. An exponential-like drop in the T_c with increasing FOV can be found in subjects A and E. In subjects A, B, and E, a significant ($p < 0.01$) decrease in T_c from the 10° FOV condition occurred within a 40° FOV.

To compare results across subjects, the mean T_c values in Fig. 4 were normalized within each subject and then combined in Fig. 5(a). A wide FOV produced a reduction in T_c of about 10–12% in most subjects compared to a 10° FOV. Most of this improvement for subjects A and E can be obtained with a FOV as small as 40° and for subjects B and D, with a FOV as small as 20°.

In contrast, the stationary peripheral visual scene produced results that were almost the opposite of the moving case. The normalized T_c data in Fig. 5(b) show that the 10° FOV condition produced the lowest mean T_c values and, with wider FOV conditions, the T_c values increased. In three subjects (B, C, and D), a 20° or 40° FOV produced a significantly ($p < 0.01$) higher T_c value than the 10° condition. For all subjects, when the moving periphery condition values are compared to the stationary ones, a significant difference is found between the T_c values at FOV's greater than 10° ($p < 0.01$). There was no significant difference in T_c values between 10° moving and stationary conditions. Results similar to these were found for the transition time constant values in the stationary periphery condition (not shown).

The filled triangles in Fig. 4 represent the mean transition time constant (T_t) for the moving case. The trend in this data follows a U-shaped curve (three of the five subjects) as the FOV increases with a minimum value at 80°. Comparing the mean T_c to the mean T_t (see Fig. 4) reveals a difference between the two that is larger at 120° than at the other FOV's in three of the five subjects (A, B, and E). Such a large difference between these two time constants signifies a much higher degree of variability in the roll error at 120° than at the other FOV's. In practical terms, the higher T_t values mean that the switch to the slower $\Delta\lambda$ took place sooner at 120° than, for example, at 80°. Despite this difference, however, all subjects were able to achieve as good a T_c value at 120° as at 80°. The normalized transition time constants (see Fig. 5(c)) show a strong U-shaped trend in all but subject D. In addition, we found that the bulk of the performance increase took place with a FOV as small as 40°.

The RMS error values in Fig. 6 show a reduction in average Stage-1 and Stage-2 RMS values with increasing FOV for three subjects. These data show a similar U-shaped relationship to FOV as did the T_t data. The normalized RMS error data, in Fig. 7, show this relationship in four of the five subjects. Most of the reduction in RMS error from the 10° condition takes place at the 40° FOV, with the minimum RMS error values between 40° to 80° FOV. Note that, for subjects C and D, who showed no significant change in T_c, both RMS error values decrease with increasing FOV.

The RMS error values for the stationary peripheral visual scene showed the same type of relationship to FOV as did its time constant data. The largest RMS error values were found at FOV's other than 10°. In four of the five subjects, the Stage-1 RMS error values peaked at 40° and were significantly different ($p < 0.01$) from those at 10°. A similar result was found for the Stage-2 RMS error data (not shown).

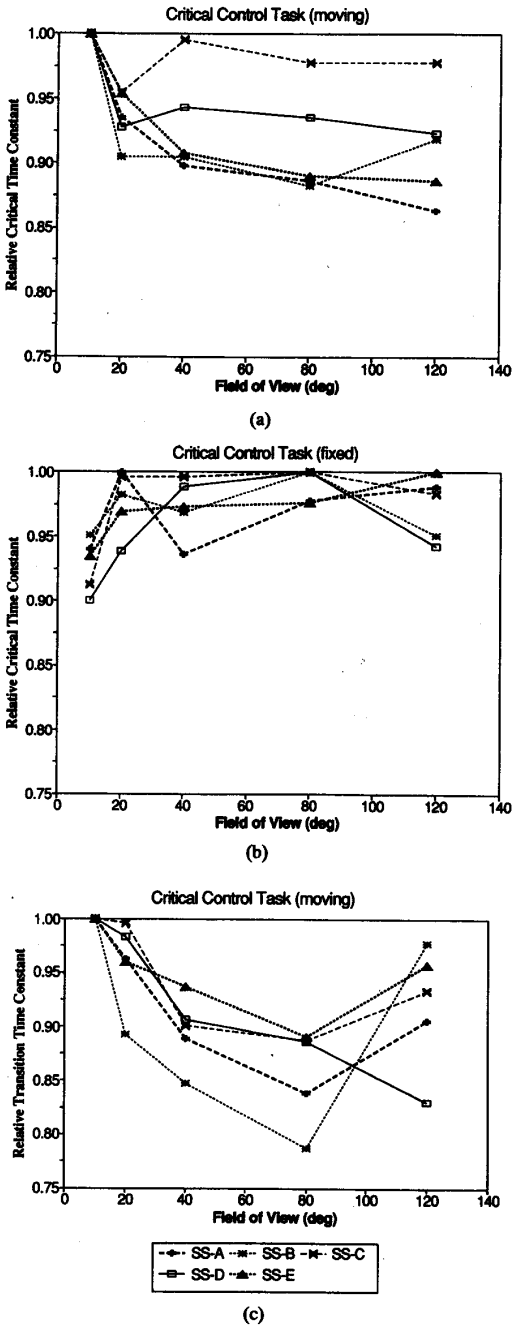

Fig. 5. Normalized time constants versus FOV from CT experiments with moving and stationary peripheral images for all subjects. (a) Critical time constant for moving peripheral images. (b) Critical time constant for stationary peripheral images. (c) Transition time constant for moving peripheral scene.

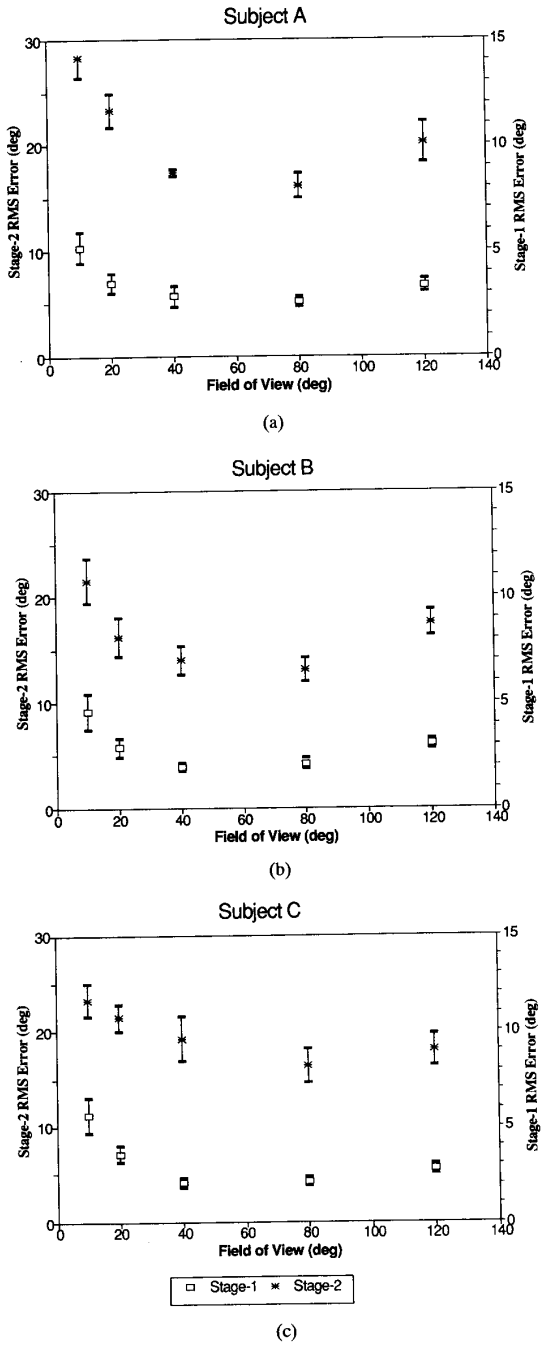

Fig. 6. Mean Stage-1 and Stage-2 performance from three subjects along with the standard deviation. Stage-2 performance is the upper set of data in all graphs.

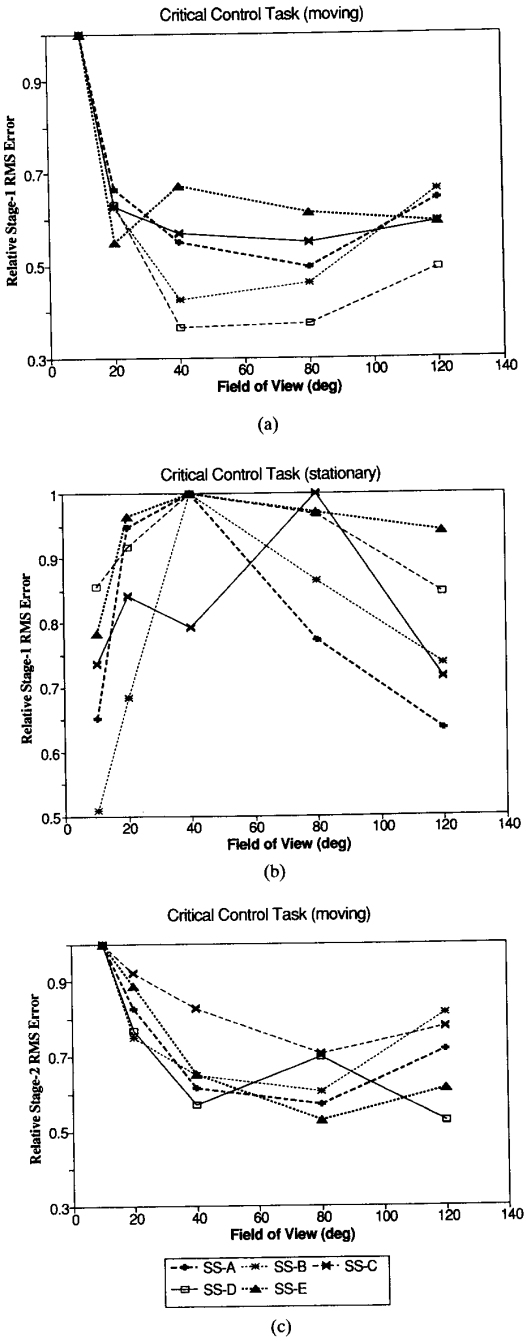

Fig. 7. Normalized Stage-1 and Stage-2 performance versus FOV from critical tracking experiments for all subjects. Stage-1 performance is from (a) the moving periphery condition and (b) the stationary periphery condition. Stage-2 performance is from (c) the moving periphery condition.

B. Subcritical Tracking Experiment

Mean RMS error values from two subjects as a function of FOV and λ along with the standard deviations are shown in Fig. 8. The RMS error values decreased by 25% in both subjects at the highest instability tested as the FOV increased from 10° to 40°. The RMS error values showed virtually no change from 40° to 120° at all λ values, except for a λ of 3.0, in subject E, where a trend for higher RMS at 120° can be seen.

At the highest λ value for each subject ($\lambda_{\max}$), increasing the FOV produced an increase in crossover frequency (ω_c).

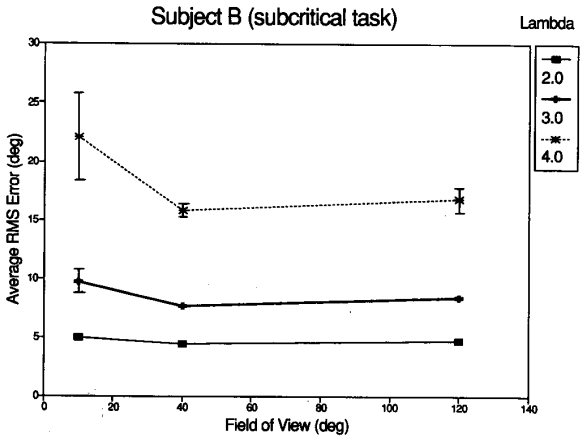

(a)

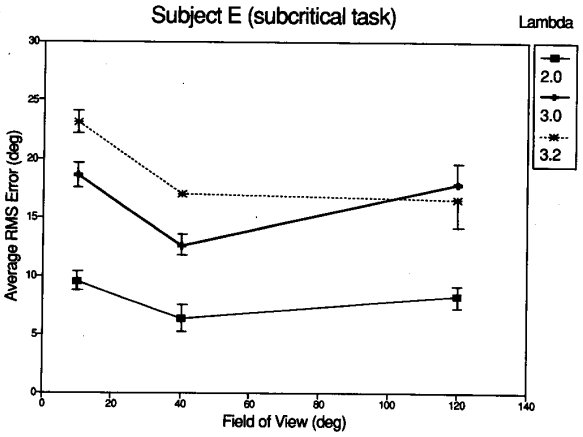

(b)

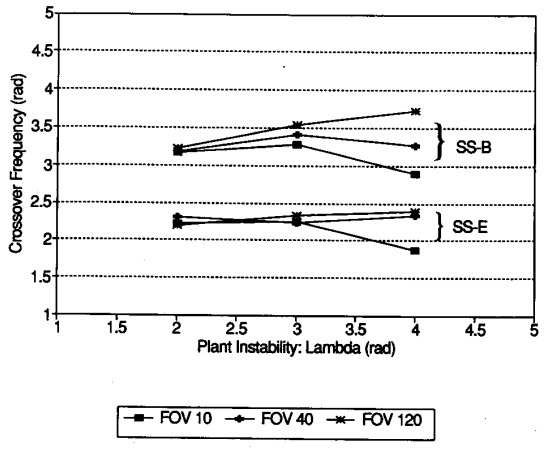

(c)

Fig. 8. (a) and (b) Average RMS error from the subcritical experiment at different FOV and λ values for two subjects. (c) Crossover frequency versus plant instability for each subject at the three FOV conditions. Note: λ_{max} was 4.0 for subject B and 3.2 for subject E.

The mean ω_c and phase margin values for each subject, along with the standard deviations, are presented in Table I. For

TABLE I
CROSSOVER FREQUENCY AND PHASE MARGIN VALUES FOR TWO SUBJECTS USING THE SUBCRITICAL TASK WITH MOVING PERIPHERAL SCENE AT THE D SETTINGS FOR EACH

SS-B			SS-E		
FOV (deg)	Wc (rad/sec)	PM (deg)	FOV (deg)	Wc (rad/sec)	PM (deg)
λ = 2.0 (rad/sec)			λ = 2.0 (rad/sec)		
10	3.17	22.09	10	2.22	13.46
40	3.18	23.77	40	2.31	20.54
120	3.22	23.55	120	2.20	17.93
λ = 3.0 (rad/sec)			λ = 3.0 (rad/sec)		
10	3.29	13.79	10	2.26	8.39
40	3.42	18.50	40	2.23	12.90
120	3.54	17.60	120	2.34	14.20
λ = 4.0 (rad/sec)			λ = 3.2 (rad/sec)		
10	2.90	14.38	10	1.88	21.10
40	3.27	13.13	40	2.34	21.09
120	3.73	16.40	120	2.39	24.09

subject B, ω_c increased 10% from 10° to 40° FOV and increased an additional 12% from 40° to 120° FOV, but it showed no real improvement in phase margin. For subject E, a 20% improvement in ω_c takes place from 10° to 40° with virtually no change from 40° to 120°. However, the phase margin increased 12% from 40° to 120° FOV. A plot of the ω_c versus λ at each FOV (see Fig. 8(c)) shows that ω_c is lowest at 10° in both subjects for all values of λ. A gradual separation of ω_c at each FOV is seen in subject B as λ increases from 3.0 to λ_{max}. In subject E, a distinct separation in ω_c is found only at λ_{max}, the result of a reduction in ω_c at the 10° FOV.

V. CONCLUSION

A human operator's performance in a disturbance nulling task with only a central FOV display can be dramatically improved if veridical motion cues are added or if the FOV is expanded to cover the peripheral retina. The addition of motion stimulates the vestibular sensors that produce lead information to aid the operator during tracking [15], [22]. Neurophysiological studies have found that visual motion in the peripheral retina can effect changes in the activity of cells that also carry vestibular motion information from the semicircular canals [23]. This suggests that presentation of images that extend into the far periphery provides the opportunity for the peripheral retina to utilize this velocity information in a manner similar to vestibularly sensed motion and, in turn, provide the human operator with lead information that can aid in stabilizing a marginally stable plant [7], [8], [13]. Our data are consistent with these previous reports on the effects of FOV and tracking. Furthermore, they show that most of the improvements in tracking performance can be obtained with only moderately sized fields of view.

Hosman and van der Vaart [7], [8] found that the "effective" time delay calculated from human operator describing functions dropped from 0.28 to 0.25 s (a 10% drop) with the addition of two peripheral displays.[5] Our results showed improvements of 10–15% in critical time constant T_c (which is a measure of "effective" time delay τ_e) with the widening of the FOV. In general, we found that a FOV of 40° is

[5]Their peripheral display began at 51° and ended at 100° into the peripheral retina on the left and 75° to 94°, on the right; the central display was 7°.

sufficient to obtain most of the reduction in T_c due to wide FOV presentations up to 120°. The sharp decline in T_c between 10° and 40° was significant in three of the five subjects.

Junker and Price [13] found that adding a pair of peripheral displays to a central display reduced RMS roll error by 27% (calculated from their Fig. 7).[6] Hosman and van der Vaart [7], [8] found an 18% decrease in the standard deviation of the error and control stick signals in their subjects with an increase in FOV. Our SC tracking RMS values show a 25% reduction at 40° and 120° FOV's as compared to 10°. In addition, if we average together the error values for all subjects at 10° FOV and then at 120° FOV for the CT experiment, we find a reduction of 40% in Stage-1 and 30% in Stage-2 RMS error values. However, we also see a steep decline in both Stage-1 and Stage-2 RMS error values across subjects for intermediate FOV conditions. In both measures, the major reduction in RMS error occurs at about 40°, with some subjects showing a further reduction out to 80°. Two subjects, who showed no significant change in T_c with wider FOV's, did show significant changes in Stage-1 and Stage-2 RMS error values with widening FOV.

The open-loop crossover frequency and phase margin show the frequency range in which the subject effectively controls the system dynamics and the relative stability of the closed-loop system. Hosman and van der Vaart [7], [8] found ω_c remained constant but the phase margin increased from 30° to 56° with the addition of peripheral displays. Our subjects showed a more varied pattern of behavior. The data at $\lambda_{\max}$ in Table I show that an increase in ω_c occurs in each subject when the FOV changes from 10° to 40° FOV with little change in phase margin. Furthermore, a 10° versus a 120° FOV shows more than a 20% increase in both ω_c and phase margin. For subject E, a FOV change from 40° to 120° shows no change in ω_c but a change in phase margin.

The variability we find in our subjects' responses when compared to the Hosman and van der Vaart data [7], [8], may be the result of our low number of subjects, and trials per subject compared to theirs. Consequently, this observed variability may be due to population sampling effects. However, examining individual subject characteristics can give insight into the tradeoffs operators make between gain and phase margin to suit some control/stability criteria. For example, if we assume the system model in (5), increasing the FOV from 10° to 120° will result in a smaller τ_e (see Fig. 4), and therefore a smaller phase lag if the tracking conditions (i.e., $\lambda_{\max}$) force the operator to always maintain the minimum possible delay. This decrease in phase lag may manifest itself in the describing function in several ways: 1) the gain K_c may remain constant and thus bandwidth as measured by ω_c is unchanged but the phase margin and stability will increase as was the case in [7], [8]; 2) the gain K_c may increase, increasing ω_c, until the same phase margin as before is acheived; and c) both gain and phase margin may be adjusted to satisfy the control/stability criteria of the operator [20], [17]. Given the difficulty of controlling our marginally unstable plant some subjects may utilize the increase in responsiveness to better maintain stability and reduce workload. Others may use it as a challenge to acheive better tracking performance. Further work in this area would be needed to make any stronger conclusions.

Recent studies have blurred the distinction between the central and peripheral visual field functions (see [24]). Previously, the visual system was thought of as having two functional areas: central for identification and peripheral for orientation [2], [4], [13]. Recently, the central FOV has been shown to produce subjective sensations that were once thought of as the exclusive domain of the peripheral field [1], [3], [11], [24]. These studies have shown the power of the central field to elicit responses that can dominate or modify the peripheral field response. Our data show that a small FOV of 10° or 20° does not yield as good an overall performance as can be found at 40° and beyond. The 40° FOV may encompass enough of the periphery so that image velocity can be utilized more effectively by the operator. In addition, the large changes in performance measures from 10° to 40°, as compared to 40° to 120°, suggest that cooperative and consistent information in both peripheral and central FOV can exert beneficial influences for the use of visual velocity information so that moderately sized FOV's can produce significant performance enhancements.

The significant differences found in the T_c and the RMS data, when a moving rather than a stationary surround is used, show that merely increasing the FOV without veridical visual motion does not aid the operator's control and may actually impede control function. In four of the five subjects, the absence of a stationary background image in the 10° FOV produced significantly better performance than when a stationary background was present. The FOV setting of the background that caused the significant reduction in performance was not uniform across subjects. However, in most subjects, performance was poorest at 20° or 40° FOV settings.

Evidence that the appearance of a stationary surround may interfere with the subject's ability to extract veridical motion information from the display has been found in other visual motion experiments. Howard and Heckmann [11] found that subjects viewing a horizontally moving central display of dots with an area equal to that of a stationary surround of dots, misinterpret the motion of the central dots as relative motion of the surround and even reported vection produced by the illusory motion of the surround. This "contrast motion vection" effect [11] appeared when the central and peripheral display areas were equal. Perhaps our result of a significant impairment in tracking with a stationary background present is related to a "contrast motion vection" effect. However, none of our subjects reported peripheral vection that might have been induced by the central visual field motion.[7] Nevertheless, this does not necessarily negate possible effects related to "motion contrast vection."

Both RMS error (Stage-1 and -2) and T_t showed an unexpected increase at 120° FOV without a commensurate increase

[6] Central display of 10° and peripheral display began at 40° and ended at 90° on both sides.

[7] Differences between their study and ours are: a) they examined circular vection not roll vection; b) their subjects were not occupied with a demanding manual control task; and c) the size of their central display was 54° × 44° square as opposed to the circular 10° central display used here.

in "effective" time delay. Our subjects' comments on comfort and ease of control more closely matched the RMS error and T_t data rather than the T_c data. They reported that the task was easiest to control at 80° FOV and noted with some amazement that the 120° FOV did not further reduce task difficulty. Thus, while subjects may be pushed by the CT paradigm to achieve a value of T_c that changes very little from 40° to 120°, the subjective reports hint that workload changes with different FOV conditions. Since a quantitative paradigm to measure workload was not included in this study, further exploration of this issue must be addressed by future experiments wherein workload is measured quantitatively.

Perhaps a factor in the increased task difficulty experienced by our subjects in the 120° FOV condition is the vection reported by our subjects in this case. Subjects reported intermittent and unpredictable episodes of vection during the conduct of these experiments, but only at the 120° FOV condition. They reported that the vection was most likely to occur at the lower λ values, when the roll velocity was relatively slow, and the amplitude was low. The fact that vection reports were primarily limited to the 120° FOV condition may be due to the demanding tracking task performed by our subjects. Brandt [2] found that consistent vection was experienced with FOV's of 60° or greater. Therefore, we would have expected vection at 80° as well as at 120°. However, our subjects' focus on the central field task may have suppressed vection sensations until a wider FOV produced a signal that was too strong to be suppressed by the concentration on the central task. We speculate that this intermittent vection might have disrupted each subject's concentration, thereby making the task more difficult to control. For example, the conflict between visual motion and vestibular no-motion information could lead to the disorientation of the subject for brief period, enough to distract him from the tracking task. Studies on simulator sickness have shown that cue conflict can result in disorientation and motion sickness symptoms [19], [14]. If a related process was at work in these experiments, then the rise in RMS error we found at 120° would be an experiment-specific degradation due to the absence of true motion of the subject. One would not expect to find this behavior under conditions where veridical vestibular motion was present, but it might appear in other wide-FOV no-motion conditions such as fixed-based flight simulators.

Finally, the possibility that the wider FOV may have introduced visual motion velocities in the far periphery that were poorly processed by that portion of the visual field seems unlikely. Although the linear velocity of an object moving at a constant angular velocity increases as the object moves farther from the center of rotation, the ability of the periphery to process these higher velocities improves as one goes farther out into the periphery [18].

ACKNOWLEDGMENT

The authors thank A. Natapoff for his help with the statistics and the design of the balanced trial presentations, N. Lambropoulos for his help in analyzing some of the data, our subjects for giving so generously of their time, L. Young and G. Zacharias for their comments during the experiments, and F. Previc and G. Agarwal for their review of the manuscript.

REFERENCES

[1] G. Andersen and M. Braunstein, "Induced self-motion in central vision," *J. Exp. Psychol.: Human Percept. Perform.*, vol. 11, pp. 122–132, 1985
[2] T. Brandt, J. Dichgans, and K. Koenig, "Differential effects of central versus peripheral vision on egocentric and exocentric motion perception," *Exp. Brain Res.*, vol. 16, pp. 476–491, 1973.
[3] B. Cheung and I. Howard, "Optokinetic torsion: Dynamics and relation to circularvection," *Vision Res.*, vol. 31, pp. 1327–1335, 1991.
[4] J. Dichgans and T. Brandt, "Visual-vestibular interaction: Effects on self-motion perception and postural control," in *Handbook of Sensory Physiology. Vol. III. Perception.*, R. Held, H. Liebowitz, and H. Teuber, Eds. Berlin: Springer-Verlag, 1978.
[5] K. Gillingham and J. Wolfe, "Spatial orientation in flight," in *Fundamentals of Aerospace Medicine*, Roy DeHart, Ed. Lea and Sebifer, 1985.
[6] R. Held, "Two modes of processing spatially distributed visual stimulation," in *The Neurosciences, Second Study Program*, F. O. Schmidt, Ed. New York: Rockefeller Univ. Press, 1970.
[7] R. Hosman and J. van der Vaart, "Effects of vestibular and visual motion perception on task performance," *Acta Psychol.*, vol. 48, pp. 271–287, 1981.
[8] —, "Motion perception and vehicle control," in *Perception and Control of Self-Motion*, R. Warren and A. Wertheim, Eds. Hillsdale, NJ: Erlbaum, 1990.
[9] E. Howlett, *Wide Angle Photography Method and System*, U.S. Pat. 4 406 532, Sept. 27, 1983.
[10] I. Howard, *Human Visual Orientation*. Toronto, ON, Canada: Wiley, 1982.
[11] I. Howard and T. Heckmann, "Circular vection as a function of the relative sizes, distances and positions of two competing visual displays," *Perception*, vol. 18, pp. 657–665, 1989.
[12] H. Jex, J. McDonnell, and A. Phatak, "A critical tracking task for man-machine research related to the operator's effective time delay. Part I: Theory and experiments with a first-order divergent control element," NASA, Tech. Rep. CR-616 (NTIS N66-39893), 1966.
[13] A. Junker and D. Price, "Comparison between peripheral display and motion information on human tracking about the roll axis," in *Proc. AIAA Visual and Motion Simulation Conf.*, Apr. 1976, pp. 26–28.
[14] R. Kellogg, C. Castore, and R. Coward, "Psychophysical effects of training in a full vision simulator," in *Proc. 51st Meeting Aerospace Med. Assoc.*, May 1980.
[15] W. Levison and A. Junker, "A model for the pilot's use of motion cues in roll axis tracking tasks," Tech. Rep. AMRL-TR-77-40 (NTIS ADA-043-690), Apr. 1977.
[16] J. McDonnell and H. Jex, "A critical tracking task for man-machine research related to the operator's effective time delay. Part II: Experimental effects of system input spectra, control stick stiffness, and controlled element order," NASA, Tech. Rep. CR-674 (NTIS N67-16012), 1967.
[17] D. McRuer, D. Graham, E. Krendel, and W. Reisener, "Human pilot dynamics in compensatory systems–Theory, models and experiments with controlled element and forcing function variations," Tech. Rep. AFFDL-TR-65-15 (NTIS AD-470-337), 1965.
[18] K. Nakayama, "Properties of early motion processing: Implications for the sensing of egomotion," in *Perception and Control of Self-Motion*, R. Warren and A. Wertheim, Eds. Hillsdale, NJ: Erlbaum, 1990.
[19] J. Reason, "Motion sickness adaptation: A neural mismatch model," *J. Roy. Soc. Med.*, vol. 71, pp. 819–829, 1978.
[20] T. Sheridan and W. Ferrell, *Man-Machine Systems*. Cambridge, MA: MIT Press, 1974.
[21] S. Siegel, *Nonparametric Statistics for the Behavioral Sciences*. New York: McGraw-Hill, 1956.
[22] R. Shirley and L. Young, "Motion cues in man-vehicle control," *IEEE Trans. Man-Machine Syst.*, vol. MMS-9, pp. 121–128, 1968.
[23] W. Waespe and V. Henn, "Neuronal activity in the vestibular nuclei of the alert monkey during vestibular and optokinetic stimulation," *Exp. Brain Res.*, vol. 27, pp. 523–538, 1977.
[24] L. Wolpert, "Field-of-view information for self-motion perception," in *Perception and Control of Self-Motion*, R. Warren and A. Wertheim, Eds. Hillsdale, NJ: Erlbaum, 1990.
[25] L. Young, "Methods and design: Survey of eye movement recording methods," *Res. Methods Instrum.*, vol. 7, pp. 397–429, 1975.

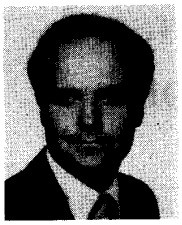

Robert V. Kenyon (S'71–M'78) received the B.S. degree from the University of Rhode Island, Kingston, in 1970, the M.S. degree in bioengineering from the University of Illinois, Chicago, in 1972, and the Ph.D. degree in physiological optics from the University of California, Berkeley, in 1978.

From 1979 to 1986, he was a faculty member of the Department of Aeronautics and Astronautics at the Massachusetts Institute of Technology, Cambridge. While there he participated in several shuttle experiments that studied the effects of microgravity on human orientation: Spacelab-1 and German Space-lab (D-1). He is currently an Associate Professor of Electrical Engineering and Computer Science at the University of Illinois at Chicago. His research interests include sensory-motor adaptation, visuomotor control, and the effects of microgravity on vestibular development, flight simulation, and computer graphics. A majority of his research has examined the contribution of visual information in the control of motor coordination.

Dr. Kenyon is a member of the ACM, Sigma Xi, and the BME Society.

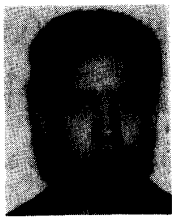

Edward W. Kneller (M'87) received the S.B. and S.M. degrees from the Department of Aeronautical and Astronautics at the Massachusetts Institute of Technology, Cambridge, in 1984 and 1986, respectively.

He is currently stationed at the Oceana Naval Air Station where he is a Navy pilot flying the F-14 Tomcat.

Lt. Kneller is a member of the AIAA.